bioRxiv preprint doi: https://doi.org/10.1101/2022.04.27.489735; this version posted April 29, 2022. The copyright holder for this preprint (which was not certified by peer review) is the author/funder, who has granted bioRxiv a license to display the preprint in perpetuity. It is made available under aCC-BY 4.0 International license.

ZW sex-chromosome evolution and contagious parthenogenesis in Artemia brine shrimp

Marwan Elkrewi[1#], Uladzislava Khauratovich[12#], Melissa A. Toups[13#], Vincent Kiplangat Bett[1], Andrea Mrnjavac[1], Ariana Macon[1], Christelle Fraisse[14], Luca Sax[15], Ann Kathrin Huylmans[16], Francisco Hontoria[7], Beatriz Vicoso[1@]

[1] Institute of Science and Technology Austria, Klosterneuburg, Austria

[2] Department of Chromosome Biology, Max Perutz Labs, University of Vienna, Vienna BioCenter, Vienna, Austria

[3] Department of Life and Environmental Sciences, Faculty of Science and Technology, Bournemouth University, Dorset, UK

[4] Univ. Lille, CNRS, UMR 8198 – Evo-Eco-Paleo, F-59000, Lille, France

[5] Lewis and Clark College, Portland, OR, USA

[6] Institute of Organismic and Molecular Evolution, Johannes Guttenberg Universität Mainz, Mainz, Castellón, Germany

[7] Instituto de Acuicultura de Torre de la Sal (IATS-CSIC), Spain

[@] bvicoso@ist.ac.at

[#] These authors contributed equally to this work.

bioRxiv preprint doi: https://doi.org/10.1101/2022.04.27.489735; this version posted April 29, 2022. The copyright holder for this preprint (which was not certified by peer review) is the author/funder, who has granted bioRxiv a license to display the preprint in perpetuity. It is made available under aCC-BY 4.0 International license.

Abstract

Eurasian brine shrimp (genus *Artemia*) have closely related sexual and asexual lineages of parthenogenetic females, which produce rare males at low frequencies. Although they are known to have ZW chromosomes, these are not well characterized, and it is unclear whether they are shared across the clade. Furthermore, the underlying genetic architecture of the transmission of asexuality, which can occur when rare males mate with closely related sexual females, is not well understood. We produced a chromosome-level assembly for the Eurasian species *A. sinica* and characterized in detail the pair of sex chromosomes of this species. We combined this with short-read genomic data for the sexual species *A. sp. Kazakhstan* and several lineages of *A. parthenogenetica,* allowing us to perform a first in-depth characterization of sex-chromosome evolution across the genus. We identified a small differentiated region of the ZW pair that is shared by all sexual and asexual lineages, supporting the shared ancestry of the sex chromosomes. We also inferred that recombination suppression has spread to larger sections of the chromosome independently in the American and Eurasian lineages. Finally, we took advantage of a rare male, which we backcrossed to sexual females, to explore the genetic basis of asexuality. Our results suggest that parthenogenesis may be partly controlled by a locus on the Z chromosome, highlighting the interplay between sex determination and asexuality.

bioRxiv preprint doi: https://doi.org/10.1101/2022.04.27.489735; this version posted April 29, 2022. The copyright holder for this preprint (which was not certified by peer review) is the author/funder, who has granted bioRxiv a license to display the preprint in perpetuity. It is made available under aCC-BY 4.0 International license.

Introduction

The diversity of reproductive and sex-determining systems has long puzzled evolutionary biologists (Bachtrog *et al.* 2014; Pennell *et al.* 2018; Picard *et al.* 2021). When separate sexes are present, the development of males and females can be controlled by environmental factors or through the presence of sex-determining loci (Beukeboom and Perrin 2014; Bachtrog *et al.* 2014). These sex determining loci are typically carried by specialized “sex chromosomes”, such as the X and Y chromosomes of mammals. Sex chromosomes initially arise from standard pairs of autosomes, but can progressively stop recombining over much of their length, ultimately resulting in genetic and morphological differentiation (Charlesworth *et al.* 2005; Wright *et al.* 2016). Each segment of the sex chromosome pair that stopped recombining at a given timepoint is referred to as a "stratum", and strata of different ages are often found on the same pair of sex chromosomes (Lahn and Page 1999; Handley *et al.* 2004). The Y chromosome stops recombining altogether after XY recombination suppression and eventually degenerates, i.e. it accumulates deleterious mutations and can lose many or even all of its genes (Bachtrog 2013). This gene loss leads to dosage deficits in males, since many X-linked genes become single-copy. Mechanisms of dosage compensation often target the X-chromosome and regulate its expression, thereby reestablishing optimal dosage balance of genes across the genome (Charlesworth 1978; Straub and Becker 2007; Vicoso and Bachtrog 2009; Disteche 2016). Much of our understanding of these processes has come from studying the ancient XY systems of traditional model organisms such as mice and fruit flies. Despite the recent characterization of young sex chromosomes in many nonmodel species (Charlesworth 2019), many questions remain about the earlier stages of sex-chromosome divergence, such as what molecular mechanisms and selective pressures drive the initial loss of recombination between sex chromosomes (Ponnikas *et al.* 2018). Similarly, female-heterogametic species (i.e. females are ZW, males are ZZ) have remained relatively understudied, as they are not found in any of the main model organisms. While parallels exist between the evolution of XY and ZW pairs, such as

bioRxiv preprint doi: https://doi.org/10.1101/2022.04.27.489735; this version posted April 29, 2022. The copyright holder for this preprint (which was not certified by peer review) is the author/funder, who has granted bioRxiv a license to display the preprint in perpetuity. It is made available under aCC-BY 4.0 International license.

the progressive loss of recombination and subsequent degradation of the Y/W-chromosomes (Ellegren 2011; Vicoso *et al.* 2013; Zhou *et al.* 2014; Picard *et al.* 2018; Sigeman *et al.* 2021), some aspects of their evolution seem to differ. In particular, dosage compensation of Z-chromosomes is often limited to a few dosage-sensitive genes (i.e. it works gene-by-gene, as opposed to the chromosome-wide mechanisms found in many XY species, (Mank 2013; Rovatsos and Kratochvíl 2021)). These discrepancies may have to do with systematic differences in selection and mutation between males and females (Vicoso and Bachtrog 2009; Ellegren 2011; Mullon *et al.* 2015), or may simply be a coincidence due to the few ZW systems characterized in detail at the molecular level (Rovatsos and Kratochvíl 2021).

Although the prevalence of sexual reproduction suggests that it offers long-term advantages, asexual lineages are found in many clades and successfully inhabit a variety of ecological niches (Toman and Flegr 2018). Transitions from sexual to asexual reproduction are frequent (Neiman et al., 2014), and can involve a diversity of mechanisms that disrupt meiosis, such as novel mutations, hybridization of closely related lineages, and polyploidization (Neiman *et al.* 2014). Asexuality can evolve from any ancestral sex-determining system, including in species with differentiated sex chromosomes, (e.g. Schwander and Crespi 2009; Jaquiéry *et al.* 2014; Mignerot *et al.* 2019), and understanding the mechanisms underlying these transitions has been a key goal of the field.

In many asexual lineages, males are occasionally produced, and can fertilize closely related sexual females, which then give rise to new asexual lineages (“contagious parthenogenesis”). These crosses have facilitated the use of traditional genetic approaches for understanding the genetic architecture of asexuality (Jaquiéry *et al.* 2014). Transitions from sexual to asexual reproduction have primarily been studied in animal species where both sexual reproduction and parthenogenesis were ancestrally part of the life cycle, either in the form of cyclical parthenogenesis or haploidiploidy (Neiman *et al.* 2014). In this case, the loss of sexual reproduction and consequent obligatory parthenogenesis is often controlled by one or only a

bioRxiv preprint doi: https://doi.org/10.1101/2022.04.27.489735; this version posted April 29, 2022. The copyright holder for this preprint (which was not certified by peer review) is the author/funder, who has granted bioRxiv a license to display the preprint in perpetuity. It is made available under aCC-BY 4.0 International license.

few loci (Lynch *et al.* 2008; Sandrock and Vorburger 2011; Eads *et al.* 2012; Jaquiéry *et al.* 2014; Aumer *et al.* 2017; Yagound *et al.* 2020). In the pea aphid, the locus controlling asexuality is found on the X-chromosome (Jaquiéry *et al.* 2014), and a locus of large effect on parthenogenesis was also found on the UV sex chromosome pair of brown algae *Ectocarpus* (Mignerot *et al.* 2019), raising interesting questions about the interplay between the ancestral sex-determining system and contagious parthenogenesis. One direct link between the two phenomena is that when asexuals are derived from an ancestral XX/XY or haplodiploid sex-determination systems, rare males can be formed through the loss of an X-chromosome (Kampfraath *et al.* 2020) or through accidental production of haploid individuals during automixis (Sandrock and Vorburger 2011). Less is known about the creation of rare males when the ancestral sex-determination system was female-heterogamety. More generally, it is unclear if sex chromosomes are a prime spot for the location of genes regulating asexual reproduction, since very few transitions have been characterized in organisms with sex chromosomes.

Brine shrimp of the genus *Artemia* have both asexual and sexual species (Abatzopoulos 2018), as well as ZW sex chromosomes with putative ancient and recent strata (Bowen 1963; De Vos *et al.* 2013; Accioly *et al.* 2015; Huylmans *et al.* 2019), making them an ideal model for addressing many of these questions. While all new world species are sexual, the Eurasian clade consists of a few sexual species (including *A. sinica, A. sp. Kazakhstan* and *A. urmiana*) and of various asexual lineages (collectively refered to as *A. parthenogenetica*, and further referred to by their location of origin; Van Stappen 2002; Maccari *et al.* 2013b). Asexuals vary in ploidy, but only diploid lineages are considered here. Originally thought of as fairly ancient, these lineages turned out to have arisen recently through hybridization between asexual lineages and individuals from or closely related to *A. sp. Kazakhstan* (Baxevanis *et al.* 2006; Maccari *et al.* 2013b; Rode *et al.* 2021). In *Artemia*, such contagious parthenogenesis can occur through the production of rare males by asexual lineages, which can fertilize closely related sexual females (Maccari *et al.* 2013a; Abatzopoulos 2018). Furthermore, asexual females can mate with males

bioRxiv preprint doi: https://doi.org/10.1101/2022.04.27.489735; this version posted April 29, 2022. The copyright holder for this preprint (which was not certified by peer review) is the author/funder, who has granted bioRxiv a license to display the preprint in perpetuity. It is made available under aCC-BY 4.0 International license.

of sexual species and produce a minority of offspring sexually (Boyer *et al.* 2021). The ZW pair of *Artemia* has been mostly studied in the American species *A. franciscana* (Bowen 1963; Parraguez *et al.* 2009; De Vos *et al.* 2013; Accioly *et al.* 2015). Both a small differentiated region and a non-recombining but largely undifferentiated region were detected, making it an interesting system to understand the first steps leading to ZW divergence (Huylmans *et al.* 2019). Gene expression in the differentiated region appears to be fully balanced between males and females, but there was limited power to detect changes due to the fragmented nature of the genome (Huylmans *et al.* 2019). Eurasian lineages also carry a ZW pair (Haag *et al.* 2017), but whether the same chromosome is used for sex determination accross the clade in not known. Because *A. parthenogenetica* reproduce through central fusion automixis (Nougué *et al.* 2015), a modified form of meiosis, which allows for loss of heterozygosity when recombination between chromosomes occurs, rare recombination events between the Z and W (which replace part of the W with its Z-linked homologous region) can lead to the creation of rare males (Nougué *et al.* 2015; Boyer *et al.* 2022). Finally, the genetic mechanisms behind asexuality, and whether the sex chromosomes play any further role in its evolution, have not yet been explored in detail.

Here, we develop several genomic resources for *Artemia* lineages, including the first chromosome-level assembly for the *Artemia* genus (*A. sinica*), as well as short-read genomic data for *A. sp. Kazakhstan* and several lineages of *A. parthenogenetica*. Using these data, we are able to provide the first in-depth characterization of sex-chromosome evolution across the genus, including identifying an ancient region shared with the American species *A. franciscana*. Finally, we find evidence that asexuality is likely partly controlled by a locus on the Z chromosome - a first in a ZW sex chromosome system.

bioRxiv preprint doi: https://doi.org/10.1101/2022.04.27.489735; this version posted April 29, 2022. The copyright holder for this preprint (which was not certified by peer review) is the author/funder, who has granted bioRxiv a license to display the preprint in perpetuity. It is made available under aCC-BY 4.0 International license.

Results

1. The ZW pair is shared by American and Eurasian *Artemia*

Two genome assemblies and a high density linkage map are currently available for the American *A. franciscana* (Jo *et al.* 2021a; Han *et al.* 2021; De Vos *et al.* 2021), but resources for the Eurasian clade are more limited, with only an *A. sp. Kazakhstan* draft genome assembly recently described in Boyer et al. (2022). The median dS between the two clades is ~0.2. We assembled a male genome of *A. sinica* using PacBio long reads (~30x) and Hi-C Illumina reads (1.5*e12 reads), yielding 1213 scaffolds with an N50 of 67.19 Mb (Sup. Fig. 1) and a total length of 1.7Gb; 85% of the sequences get assigned to one of the 21 largest scaffolds (which corresponds to the expected number of chromosomes, Sainz-Escudero *et al.* 2021). The strong diagonal in the heatmap of the Hi-C contact matrix (Sup. Fig. 2) supports the high quality of our assembly, as does our BUSCO score of 91.8%. This chromosome-level assembly represents an improvement over existing *Artemia* genomes, which have N50 values of 27 to 112Kb, and BUSCO scores of 68.3% to 86.9% (Jo *et al.* 2021a; De Vos *et al.* 2021; Boyer *et al.*; Sup. Fig. 3).

Our earlier analysis of female and male genomic coverage in *A. franciscana* had uncovered a small region of reduced female coverage, consistent with full differentiation of the Z and W chromosomes (Huylmans *et al.* 2019). To investigate whether ZW differentiation was also present in *A. sinica*, we first estimated male and female coverage along each chromosome. Consistent with *A. franciscana*, only a small genomic region on chromosome 1 had decreased female/male coverage (Fig. 1A, Sup. Fig. 4 for all chromosomes), showing that chromosome 1 is the Z chromosome. To check for homology with the *A. franciscana* differentiated region, we mapped the scaffolds from the *A. franciscana* genome of (Jo *et al.* 2021a) to the new *A. sinica* assembly based on their shared gene content, and plotted the coverage values that we had previously estimated (Huylmans *et al.* 2019) based on the *A. sinica* coordinates. Fig. 1A shows that the two differentiated regions largely overlap, supporting the ancestry of the pair of sex

bioRxiv preprint doi: https://doi.org/10.1101/2022.04.27.489735; this version posted April 29, 2022. The copyright holder for this preprint (which was not certified by peer review) is the author/funder, who has granted bioRxiv a license to display the preprint in perpetuity. It is made available under aCC-BY 4.0 International license.

chromosomes; we name this shared region stratum 0 (S0). In the *A. franciscana* linkage map (Han *et al.* 2021), LG6 was identified as the sex chromosome. To further verify the homology between the ZW pairs of the two species, we mapped the genetic markers used by Han et al. (2021) to our *A. sinica* assembly. As expected, the vast majority of LG6 markers for which we could infer a location mapped to our chromosome 1 (Sup. Fig. 5). We also produced an assembly based on female long PacBio reads, which contains a substantial amount of scaffolds with excessive female coverage, consistent with W-linkage (Sup. Fig. 6).

2. Convergent loss of ZW recombination

To identify parts of the sex chromosomes that no longer recombine, but are still similar enough that W-derived reads still map to the Z, we used previously published RNA-seq dataset for *A. sinica* (Huylmans *et al.* 2021), obtained from 10 males and 10 females, to estimate FST, a measure of genetic differentiation, between the two sexes. Genetic variants found exclusively on the W increase the level of female-male differentiation, and young non-recombining regions can be detected through their high male:female FST (Palmer *et al.* 2019; Vicoso 2019; Gammerdinger *et al.* 2020). Fig. 1B shows that a large region (~52 Mb) has FST values systematically above the 95th-percentile of autosomes, consistent with recent loss of recombination in *A. sinica*. We call this region Stratum 1 (S1), but further divide it into S1a, which shows localized drops in female:male coverage (gray shaded regions in Fig. 1A), and S1b, for which no coverage differences are observed (Fig. 1A).

Given the substantial distance between the two lineages, we hypothesized that the loss of recombination in S1 had occurred specifically in the Eurasian clade. To verify this, we used a k-mer-based pipeline combining male and female DNA and RNA short reads (Elkrewi *et al.* 2021) to identify putative W-derived transcripts. This yielded 402 transcripts in *A. franciscana* and 319 in *A. sinica*. Of those that mapped to the genome, 182 out of 310 (59%) *A. sinica* transcripts and 168 out of 364 (46%) *A. franciscana* transcripts mapped to chromosome 1 (Z) of *A. sinica*, a

bioRxiv preprint doi: https://doi.org/10.1101/2022.04.27.489735; this version posted April 29, 2022. The copyright holder for this preprint (which was not certified by peer review) is the author/funder, who has granted bioRxiv a license to display the preprint in perpetuity. It is made available under aCC-BY 4.0 International license.

197 higher proportion than the overall 7% of genes that map to this chromosome, confirming the
198 validity of the approach (since we expect many W-linked genes to have a close homolog on the
199 Z). Few of these candidate W genes mapped to the putative ancestral sex-linked region (16 in
200 *A. sinica*, compared to 84 genes in the corresponding Z-linked region), consistent with
201 substantial degeneration of this part of the W-chromosome. To find genes present on the W-
202 chromosomes of both species, we selected reciprocal best hits between the two sets of W
203 candidates. Surprisingly, 15 were found in both species, but mapped to the putative S1a region,
204 suggesting that at least part of this region has also stopped recombining in *A. franciscana*. We
205 made phylogenetic trees using each pair of homologous W-genes and their Z-linked homologs
206 (as well as the closest homolog obtained from the transcriptome of the distantly related fairy
207 shrimp *Branchinecta lindahli* (Schwentner *et al.* 2018), when one could be detected, to infer
208 whether they were W-linked before the split of the two clades. ZW homologs clustered by
209 species rather than by chromosome (Fig. 1C shows two examples and the others are shown in
210 Sup. Fig. 7), showing that loss of recombination occurred independently and convergently for
211 this region in the American and Eurasian lineages.
212

bioRxiv preprint doi: https://doi.org/10.1101/2022.04.27.489735; this version posted April 29, 2022. The copyright holder for this preprint (which was not certified by peer review) is the author/funder, who has granted bioRxiv a license to display the preprint in perpetuity. It is made available under aCC-BY 4.0 International license.

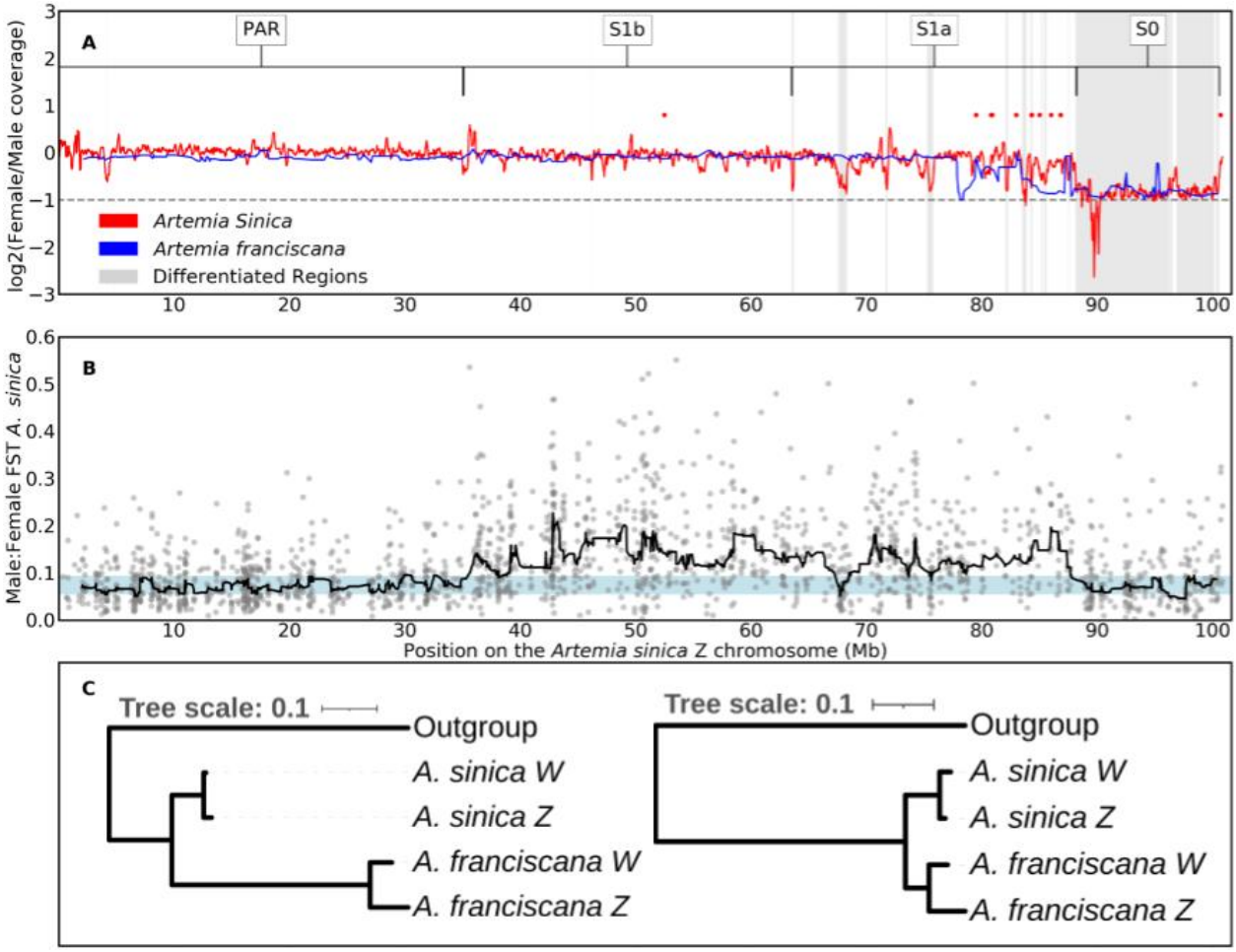

Fig.1: A shared sex-linked region on the ZW pair. A. Patterns of female/male coverage in *A. franciscana* and *A. sinica*. The differentiated regions are highlighted in gray, and the putative strata are defined above. The red dots are the locations of the W-candidates shared between *A. sinica* and *A. franciscana*. The horizontal gray line is at -1 to signify the regions with a twofold reduction in coverage in females compared to males. B. Male:female FST along the putative chromosome Z. The dots are FST calculated for bins of 1000 nucleotides, and the black line is the rolling median computed in sliding windows of 30 consecutive 1000 nucleotide bins. The light blue shaded area highlights the region between the 5th and 95th-percentiles of the rolling median of FST for autosomes. C. Phylogenetic trees for two examples of the W-candidates shared between *A. sinica* and *A. franciscana* and their putative Z homologs. *Branchinecta lindahli* is used as the outgroup.

3. Dosage compensation of the Z-specific region

Many female-heterogametic species lack a chromosome-wide mechanism of dosage compensation, and investigating the few cases that have it may shed light on the difference between ZW and XY systems. Earlier work suggested that the Z-specific region of *A.*

bioRxiv preprint doi: https://doi.org/10.1101/2022.04.27.489735; this version posted April 29, 2022. The copyright holder for this preprint (which was not certified by peer review) is the author/funder, who has granted bioRxiv a license to display the preprint in perpetuity. It is made available under aCC-BY 4.0 International license.

franciscana was compensated (Huylmans *et al.* 2019), but misidentification of genes in the sex-linked region (as the genome was fragmented) could have hidden differences between chromosomes. We repeated this analysis using RNA-seq data from thorax, head, and gonad of *A. sinica* (Huylmans et al. 2021). We first assembled a male transcriptome from all pooled male reads available for this species (to avoid hybrid assemblies of Z and W homologs, see Sup. Fig. 8 for a BUSCO assessment), mapped it to the genome assembly, and estimated expression for each sample. In somatic tissues, the female:male ratio is similar for the autosomes and each of the Z-chromosome regions ($p>0.05$, Fig. 2B and 2C), confirming that dosage compensation is active in this clade. A small shift towards male-biased expression can be observed for the S0 in gonads (Fig. 2D). Such differences in the gonad have been found even in animals with well-characterized chromosome-wide mechanisms of dosage compensation, such as Drosophila (Meiklejohn et al. 2011) and silkworm (Huylmans et al. 2017). While compensation mechanisms may be absent or less active in the gonad (Meiklejohn et al. 2011), differences could also result from the unusual regulation of the sex chromosomes in the germline (Argyridou and Parsch 2018), where they are often inactivated or downregulated (Vibranovski et al. 2009). Overall, our patterns generally support the presence of complete dosage compensation throughout the differentiated region in somatic tissues, and at least partial compensation in the gonad.

bioRxiv preprint doi: https://doi.org/10.1101/2022.04.27.489735; this version posted April 29, 2022. The copyright holder for this preprint (which was not certified by peer review) is the author/funder, who has granted bioRxiv a license to display the preprint in perpetuity. It is made available under aCC-BY 4.0 International license.

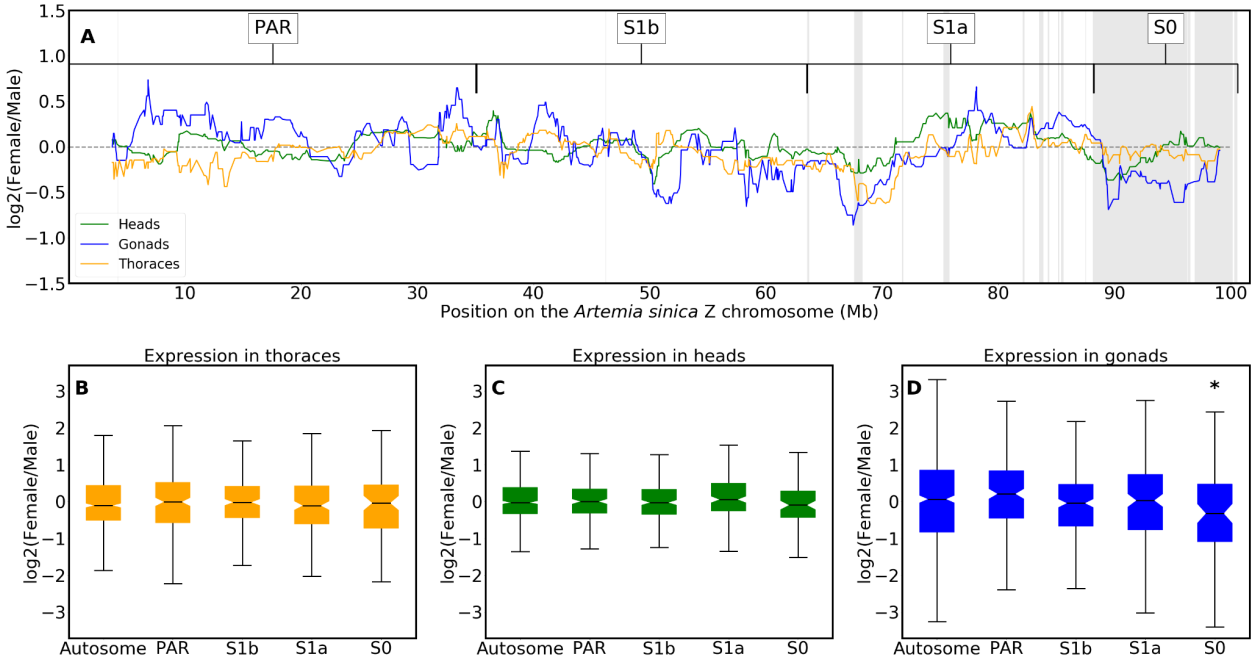

Figure 2. Dosage compensation of the Z-chromosome. Panel A: The logged ratio of female to male expression along the Z chromosome in heads, gonads and thoraces (computed as the rolling median in sliding windows of 30 consecutive genes). Gray areas represent the differentiated regions identified in the coverage analysis, and the putative strata are denoted above.The dashed horizontal black line is at zero. Panels B-D: The distribution of logged ratio of female to male expression for the autosomes and the different regions of the Z chromosome in thoraces (A), heads (B) and gonads (C).

4. The sex chomosomes of asexual females and the genetic origin of rare males

In order to characterize the ZW pair of asexual females, we first obtained a draft genome assembly of the closely related sexual species *A. sp. Kazakhstan* from illumina short reads, and estimated genomic coverage using two female and two male samples of this species. The genomic scaffolds were mapped to the *A.sinica* genome based on their gene content, and median coverages of male and female *A. sp. Kazakhstan* individuals were plotted along the *A. sinica* Z chromosome using a sliding window of 10 scaffolds (green and yellow lines in Fig. 3A). As expected, an approximately two-fold drop in female coverage was observed in a similar region to that found in *A. sinica* (marked by gray shading), whereas the male harbored high genomic coverage throughout the chromosome, consistent with the presence of the same pair

bioRxiv preprint doi: https://doi.org/10.1101/2022.04.27.489735; this version posted April 29, 2022. The copyright holder for this preprint (which was not certified by peer review) is the author/funder, who has granted bioRxiv a license to display the preprint in perpetuity. It is made available under aCC-BY 4.0 International license.

of sex chromosomes in this lineage (a similar pattern was observed in *A. urmiana*, Sup. Fig. 9). We used the *A. sp. Kazakhstan* draft genome to map genomic reads derived from three closely related asexual females (one from the Lake Urmiana-derived population, and two from a population derived from Aibi Lake cysts). In every case, the patterns of coverage were very similar to those of the *A. sp. Kazakhstan* sexual female, confirming that asexual females carry the same pair of ZW chromosomes.

Boyer *et al.* (2022) recently showed that *Artemia* rare males can be produced by ZW recombination events at variable locations near the sex-determining locus. We obtained a rare male from an *A. parthenogenetica* line from Aibi Lake (which we use in the next section to explore the transmission of asexuality). To test whether it arose through ZW recombination or other chromosomal changes, we first compared patterns of genomic coverage to those of females. No reduced coverage was observed along the Z-chromosome, arguing against the loss of a sex chromosome. We further called Single Nucleotide Polymorphisms (SNPs) in the rare male and in its sister (marked as Aibi female 2 in Fig 3A), and estimated the proportion of heterozygous SNPs present in the asexual female that were lost in the rare male. Loss of heterozygosity was detected throughout the distal half of the Z-chromosome (Fig. 3B and Sup. Fig. 10), confirming that a large part of the W was replaced by its Z homologous region. Finally, the rare male had high heterozygosity levels on other chromosomes (Sup. Fig. 11), arguing against the accidental occurrence of a version of automixis that eliminates variants across the genome (another hypothesis for the origin of rare males, Nougué *et al.* 2015). Taken together, these results support rare ZW recombination as the source of the Aibi Lake rare male (Nougué *et al.* 2015; Boyer *et al.* 2022).

bioRxiv preprint doi: https://doi.org/10.1101/2022.04.27.489735; this version posted April 29, 2022. The copyright holder for this preprint (which was not certified by peer review) is the author/funder, who has granted bioRxiv a license to display the preprint in perpetuity. It is made available under aCC-BY 4.0 International license.

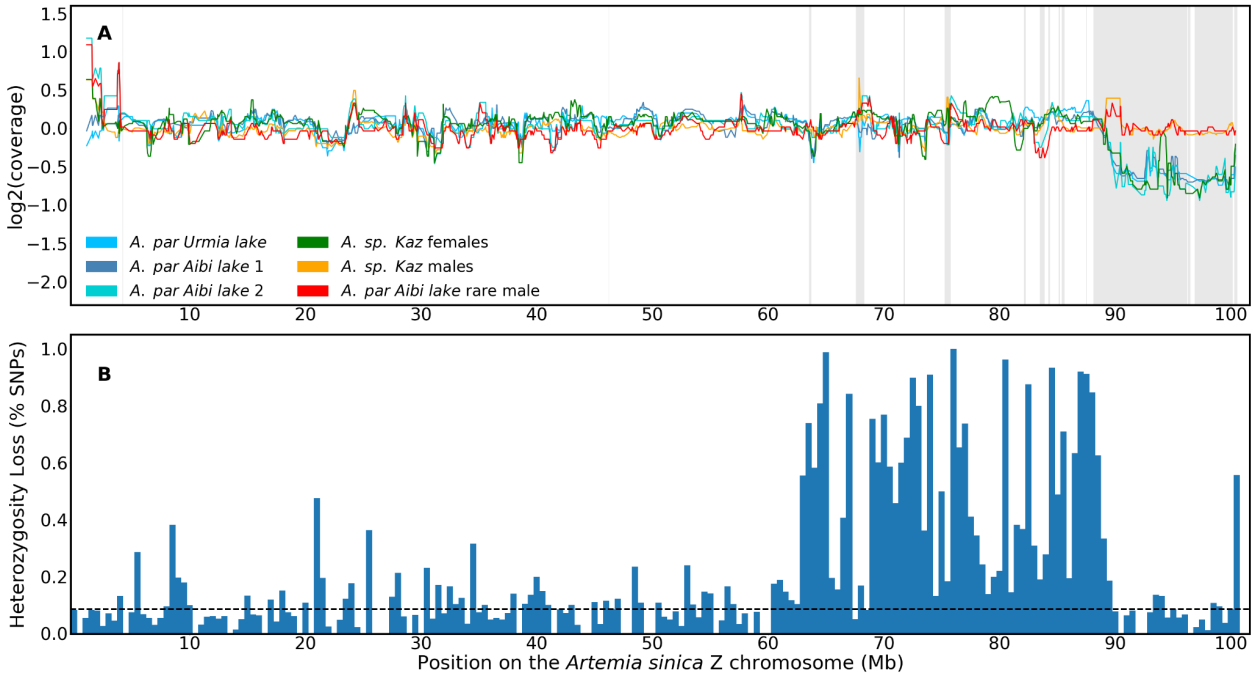

Fig. 3: The sex chromosomes of sexual and asexual individuals. A. Coverage patterns in *A. sp. Kazakhstan* male and female samples, in three asexual females, and in a rare male derived from an asexual lineage from Aibi Lake. B. The fraction of SNPs that lost heterozygosity on the rare male Z chromosome relative to its asexual sister in bins of 500Kb. The dotted line represents the average loss of heterozygosity for autosomes.

5. The Z chromosome likely contributes to the transmission of asexuality

In order to find possible loci responsible for the spread of asexuality in brine shrimp, we crossed the rare male described in the previous section and a female from *A. sp. Kazakhstan* (Sup. Fig. 12). This produced 22 asexual females and 24 males in the F1; a single female died without producing offspring asexually. The presence of asexual females in the F1 shows that the locus controlling asexuality in this lineage works in a dominant manner, unlike what was first observed in Maccari *et al.* (2014), but consistent with the recent experiments of Boyer *et al.* (2021). The fact that almost all females produced offspring without mating further suggests that the locus was likely present on both copies of the genome of the original rare male. We then backcrossed 12 males from the F1, which should only carry one copy of the locus/loci controlling asexuality, with females from an *A. sp. Kazakhstan* inbred line (of these only 6 yielded progeny). The resulting F2 generation consisted of 84 (~45%) males, 5 (~3%) asexual

bioRxiv preprint doi: https://doi.org/10.1101/2022.04.27.489735; this version posted April 29, 2022. The copyright holder for this preprint (which was not certified by peer review) is the author/funder, who has granted bioRxiv a license to display the preprint in perpetuity. It is made available under aCC-BY 4.0 International license.

311 females, and 96 (~52%) females that did not produce asexually 133 days after the crosses were
312 set up (44 individuals died before sexing was possible and are not included in the counts). We
313 presume that most of these are sexual females for our analyses, but some could have
314 reproduced asexually had the experiment been continued longer.

315 We produced whole-genome resequencing data for the 5 F2 asexual females and 10 F2
316 putatively sexual females. These were first pooled into an asexual pool and a putatively sexual
317 pool, and we used Popoolation2 to compute FST between these two pools of females. While a
318 few small peaks of FST are found on the autosomes (Fig 4a), the strongest signal comes from
319 the distal end of the Z chromsome (Fig 4b). We further predicted that loci underlying asexuality
320 should have been inherited from the original rare male by all the F2 asexual females, but not by
321 (all) control females. To test this, we mapped all DNA samples individually to the *A. sp.*
322 *Kazakhstan* genome. We also mapped the original rare male and its *A. parthenogenetica* sister,
323 and two *A. sp. Kazakhstan* individuals, in order to select SNPs that were alternatively fixed
324 between the two lineages. We used these informative SNPs to reestimate FST between F2
325 asexual and control females, and to infer which genomic regions were inherited from the rare
326 male by each of the F2 individuals. Sup. Fig. 13 shows that we recover a region of high FST on
327 the Z chromosome, and that all asexuals carry genetic material from the rare male in this region,
328 as expected if it controls asexuality. In total, only 17 scaffolds show ancestry patterns consistent
329 with an asexuality locus (i.e. they show evidence of *A. parthenogenetica* ancestry in all asexual
330 females, but not in all control females). Eleven are on the Z chromosome (versus 1 expected,
331 p=1.3e-20 with a Chi-square test), and correspond to the region of high FST, providing further
332 support for a role of the Z chromosome in the transmission of asexuality. None of the other
333 minor peaks of FST are in regions with ancestry patterns consistent with asexuality loci (Sup.
334 Fig. 13), although chromosome 6 contains 3 such loci (versus 0.9 expected, $p<0.01$ with a chi-
335 square test).

336

bioRxiv preprint doi: https://doi.org/10.1101/2022.04.27.489735; this version posted April 29, 2022. The copyright holder for this preprint (which was not certified by peer review) is the author/funder, who has granted bioRxiv a license to display the preprint in perpetuity. It is made available under aCC-BY 4.0 International license.

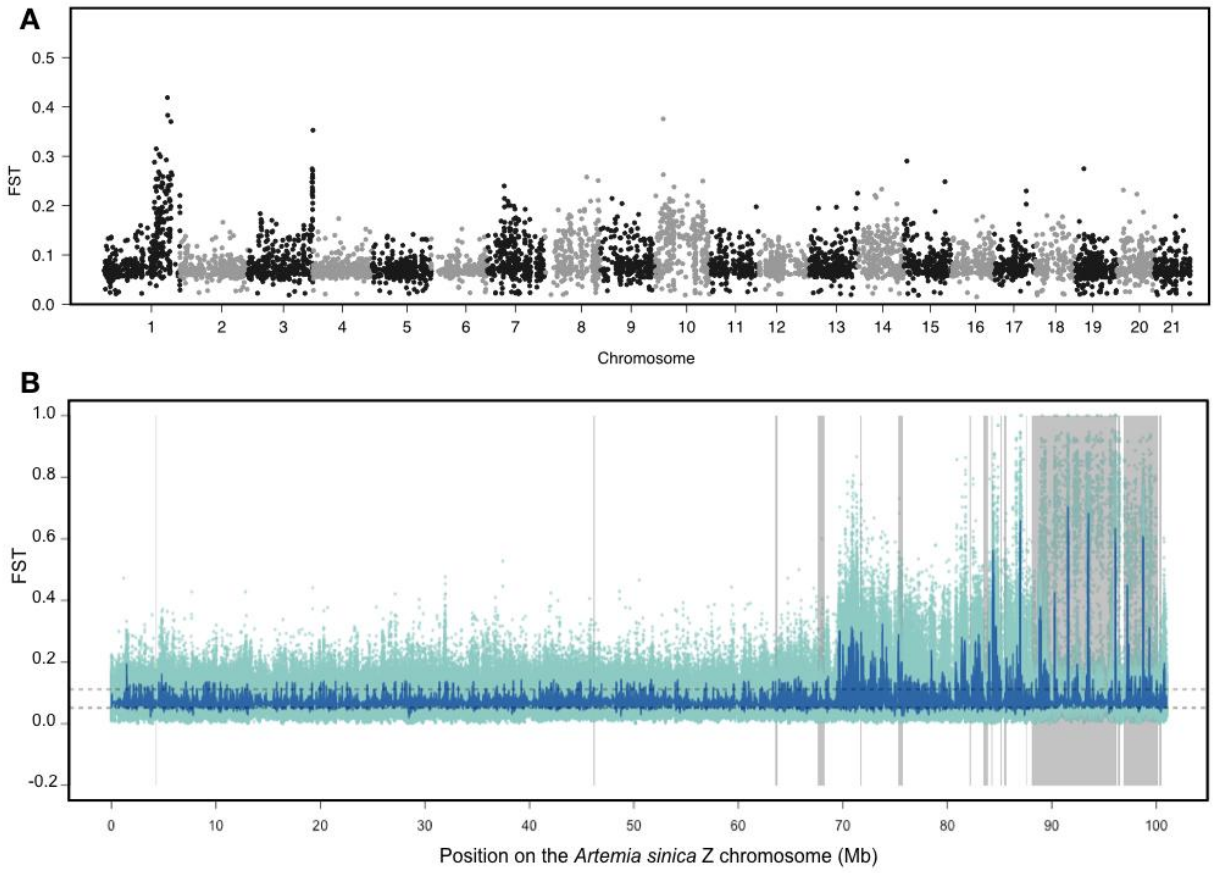

Fig 4. Elevated FST between sexual and asexual females localizes to the non-recombining region of the Z chromosome. A. Manhattan plot of FST estimated for 1Kb sliding windows between asexual and sexual females across the genome. B. FST across chromosome 1. FST is shown for individual SNPs in light green, and the blue line shows the rolling median for 101 SNPs.

Discussion

Because of their unusual ecology (Gajardo and Beardmore 2012) and ease of maintenance in the lab, *Artemia* have for decades been used as model organisms for various purposes, including toxicity screening and ecological monitoring (Rajabi *et al.* 2015; Ntungwe N *et al.* 2020; Chan *et al.* 2021; Okumu *et al.* 2021), investigating molecular mechanisms of stress resistance (MacRae 2003), and even space research (Spooner *et al.* 1992). However, their potential as models for ZW chromosome evolution and comparative genomics in general was until recently hampered by a lack of genomic resources. The publication of two genomes for the

bioRxiv preprint doi: https://doi.org/10.1101/2022.04.27.489735; this version posted April 29, 2022. The copyright holder for this preprint (which was not certified by peer review) is the author/funder, who has granted bioRxiv a license to display the preprint in perpetuity. It is made available under aCC-BY 4.0 International license.

American *A. franciscana* has already shed new light on how these charismatic organisms survive in their extreme environments (Jo *et al.* 2021a; De Vos *et al.* 2021), but no information on sex linkage was provided, and the lack of a close outgroup sequence (other than the distant Daphnia) made comparative analyses difficult. A draft genome was recently described for *A. sp. Kazakhstan* (Boyer *et al.* 2022), but there was limited power to assign scaffolds to the sex chromosomes or autosomes.

Here, we obtain the first chromosome-level assembly in the clade for the Eurasian brine shrimp *A. sinica*, and characterize in detail the differentiated and undifferentiated regions of the ZW pair. By combining these results with those of a preliminary analysis in *A. franciscana* (Huylmans *et al.* 2019), we confirmed the putative evolutionary model for the ZW pair, with an ancient well-differentiated region that stopped recombining in the ancestor of the two lineages, and more recent "strata" arising in each lineage independently. The independent loss of recombination in American and Eurasian species provides a unique opportunity to investigate convergent changes that occur in early sex-chromosome evolution. In agreement with previous findings in *A. franciscana*, *A. sinica* males and females have similar somatic expression patterns of Z-linked genes in the differentiated region which strongly supports the presence of a mechanism of dosage compensation in this group. Currently, no tractable lab model exists for the early evolution of ZW chromosomes, and Z-chromosome dosage compensation is only understood in detail for the silkworm (Walters and Hardcastle 2011; Kiuchi *et al.* 2014; Katsuma *et al.* 2019; Rosin *et al.* 2022), making this an outstanding new model clade for investigating these topics.

Finally, we obtained several putative W-genes in both species using a k-mer based analysis. Few of them mapped to the ancestral part of the W chromosome: only ~20% of the Z-linked genes in this region have a W-homolog, suggesting that much of the ancestral gene content has been lost. All of the genes for which a W-homolog could be found in both *A. sinica* and *A. franciscana* mapped to younger strata of the ZW pair, and appear to have become W-linked

bioRxiv preprint doi: https://doi.org/10.1101/2022.04.27.489735; this version posted April 29, 2022. The copyright holder for this preprint (which was not certified by peer review) is the author/funder, who has granted bioRxiv a license to display the preprint in perpetuity. It is made available under aCC-BY 4.0 International license.

independently in the two lineages. If the ancestral sex-determination mechanism is still shared by the two species, this may suggest that the primary signal for sex determination is a dosage-dependent gene on the Z rather than a dominant female-determining gene on the W. However, it is also possible that the sex-determining gene is only expressed early in development, and was missed by our analysis of adult tissues. Future studies of sex-specific expression throughout the life cycle and complete assemblies of the W chromosome of the two species will be necessary to shed light on sex determination in this group.

The proximity of *A. sinica* to the *A. sp. Kazakhstan* group, which contains both sexual and asexual populations, also allowed to characterize sex-linked sequences in this group. First, we found that the sex chromosome pair is shared by all populations. We further confirmed that rare males in this group can be produced through the replacement of the W-specific region with its Z-counterpart. Finally, our backcrossing experiment points to a role of the sex chromosome pair in the spread of asexuality through rare males.

It should be noted that this experiment has several drawbacks. First, it is difficult to phenotype females as sexual or asexual, as the timing at which asexuals produce their first brood can vary. Furthermore, hybrid incompatibilities may stop females from producing viable offspring even if they carry the alleles encoding asexuality. The fact that only ~5% of females were asexual in the F2 suggests that either the trait is polygenic, and/or that we are mistakenly classifying asexuals as putative sexuals. Finally, we only obtained a small number of backcrossed asexual females, which limits the power to infer causal loci.

Despite these drawbacks, the Z chromosome showing the strongest signal of differentiation between asexual and control females is intriguing, and in line with results in the pea aphid, which carries the asexuality locus on the X chromosome. In species where asexuality is triggered by an endoparasite such as Wolbachia, the acquisition of asexuality is thought to be driven by the transmission advantage gained by the female-transmitted parasite (since asexual reproduction leads to an all-female progeny). It is possible that an asexuality gene found on a Z

bioRxiv preprint doi: https://doi.org/10.1101/2022.04.27.489735; this version posted April 29, 2022. The copyright holder for this preprint (which was not certified by peer review) is the author/funder, who has granted bioRxiv a license to display the preprint in perpetuity. It is made available under aCC-BY 4.0 International license.

chromosome similarly benefits from a transmission advantage. If rare males always arise through the replacement of the W-specific region with its Z homolog region, a Z-linked asexuality locus will be homozygous and therefore transmitted to all daughters in the F1 (and to all sons). More detailed studies of transmission of asexuality in this group and others with ZW and XY sex chromosomes will in the future shed light on the relationship between sex determination and the rise and spread of asexual reproduction under various sex-determining mechanisms.

Materials and methods

Data availability statement

All genomic reads generated for this study are available at the NCBI short reads archive under Bioproject number XXX [*will be provided before publication*]. The pipelines used to analyze the data are at https://git.ist.ac.at/bvicoso/zsexasex2021, and important processed data files such as the new *A. sinica* genome assembly are provided in the Supplementary Materials. *[A permanent URL in the ISTA Data Repository will be provided before publication.]*

Sampling and DNA extractions

Cysts from *A. sinica* (originally from Tanggu salterns, PR China), *A. sp. Kazakhstan* (originally from an unknown location in Kazakhstan), and two lineages of *A. parthenogenetica* (from Lake Aibi (PR China) and from Lake Urmia (Iran)) were obtained from the Instituto de Acuicultura de Torre de la Sal (C.S.I.C.) Artemia cyst collection in Spain, as described in Huylmans *et al.* (2021). Cysts were hatched under 30 g/L salinity and grown to adulthood under 60 g/L salinity. Some of these F0 individuals were used directly for DNA extractions with the Qiagen DNeasy Blood & Tissue kit. We also set up iso-female lines in *A. sinica* and *A. sp. Kazakhstan*, and subjected them to 6 generations of sib-sib mating to reduce the amount of heterozygosity. Male and female individuals from *A. sinica* and *A. sp. Kazakhstan* inbred iso-

bioRxiv preprint doi: https://doi.org/10.1101/2022.04.27.489735; this version posted April 29, 2022. The copyright holder for this preprint (which was not certified by peer review) is the author/funder, who has granted bioRxiv a license to display the preprint in perpetuity. It is made available under aCC-BY 4.0 International license.

female lines were used individually for DNA extractions with Qiagen DNeasy Blood & Tissue kit. Furthermore, 20 males and 17 females of *A. sinica* (also from the inbred iso-female line) were pooled and high molecular weight DNA was extracted using the Qiagen Genomic-tip 20/G kit.

Crossing design to identify the asexuality locus

We designed a backcross in order to investigate the loci controlling asexuality (Fig S12). An asexual female from Aibi Lake produced a rare male. We crossed this male with an inbred female from the closest related sexual species, *A. sp. Kazakhstan*. This produced asexual females and males in the F1 generation. We then backcrossed 12 males from the F1 to sexual females from the same inbred line of *A. sp. Kazakhstan*. Of these, 6 crosses produced offspring, yielding a total of 84 males, 5 asexual females, and 96 putatively sexual females (those that did not reproduce asexually for 133 days after the crosses were set up). The 5 asexual females and 10 control females were used individually for DNA extractions with the Qiagen DNeasy Blood & Tissue kit. The control females came from the same crosses (i.e. had the same F2 father and *A. sp. Kazakhstan* mothers) as the asexual females, but were otherwise selected randomly.

DNA short and long read sequencing

PacBio libraries were prepared and sequenced at the Vienna Biocenter Sequencing facility for the male and female *A. sinica* high molecular weight DNA. All other DNA samples were used for Illumina paired-end sequencing. Libraries were prepared and sequenced at the Vienna Biocenter Sequencing Facility. Finally, 1 male was frozen and provided to the sequencing facility for Hi-C library preparation and Illumina sequencing on a NovaSeq machine. The final list of samples, as well as the parts of the analysis that they were used in, are listed in Sup. Table 3.

Genome assemblies

bioRxiv preprint doi: https://doi.org/10.1101/2022.04.27.489735; this version posted April 29, 2022. The copyright holder for this preprint (which was not certified by peer review) is the author/funder, who has granted bioRxiv a license to display the preprint in perpetuity. It is made available under aCC-BY 4.0 International license.

456 The male PacBio reads were assembled using two different genome assemblers: Flye
457 v.2.7.1, (Kolmogorov *et al.* 2019) and Miniasm [0.3-r179, minimap2 2.18-r1028-dirty was used
458 for mapping and the consensus was generated using Racon v1.4.22](Li 2016; Vaser *et al.*
459 2017). The Flye assembly was polished using male *Artemia sinica* short genomic reads
460 (trimmed with the Trimmomatic package, Bolger *et al.* 2014), and the Miniasm assembly was
461 polished using the same male short reads using the wtpoa-cns tool from wtdbg2 v.2.5 (Ruan
462 and Li 2020). The two assemblies were then merged using quickmerge v.0.3 (Chakraborty *et al.*
463 2016) with the Miniasm assembly as the query and the Flye assembly as the reference. The
464 resulting assembly was purged using the purge_dups program v.1.2.5 (Guan *et al.* 2020)).
465 To scaffold the assembly into pseudo-chromosomes, the PCR duplicates were first removed
466 from the Hi-C data using the clumpify.sh script from the bbmap package (Bushnell 2014), and
467 the Hi-C reads were then mapped to the genome assembly using the Arima mapping pipeline
468 with MAPQ 5 (Arima Genomics 2021) and then scaffolded using the YaHS tool (pre-release of
469 version 1.1, Zhou 2022). The contact maps were visualized and manually edited on Juicebox
470 v.1.11.08, Robinson *et al.* 2018) to generate the final chromosome-level assembly.
471 The female *Artemia sinica* genome was assembled from female PacBio reads using Flye
472 (v.2.7.1), and it was not polished to avoid collapsing the Z and the W scaffolds. The *Artemia sp.*
473 *Kazakhstan* genome was assembled from two male short read libraries with Megahit v1.1.4 (Li
474 *et al.* 2015) and then scaffolded using SOAPdenovo-fusion (SOAPdenovo2 v.2.04, Luo *et al.*
475 2012).
476 BUSCO v.5.2.2, (Manni *et al.* 2021) was used to assess the completeness of the genomes
477 generated in this study and the two previously published *Artemia franciscana* genomes in the
478 genome mode with the arthropoda dataset (arthropoda_odb10).
479
480
481 **Estimation of genomic coverage**

bioRxiv preprint doi: https://doi.org/10.1101/2022.04.27.489735; this version posted April 29, 2022. The copyright holder for this preprint (which was not certified by peer review) is the author/funder, who has granted bioRxiv a license to display the preprint in perpetuity. It is made available under aCC-BY 4.0 International license.

The short genomic reads were mapped to the genome using bowtie2 v.2.4.4 (Langmead and Salzberg 2012 p. 2). The uniquely mapped reads were then extracted from the output sam files using (grep -vw "XS:i"). SOAP.coverage v.2.7.7 (Luo *et al.* 2012) was then used to calculate the coverage for each library either using 10000 bp windows (*A. sinica*) or per scaffold (other species).

Mapping of the *A. franciscana* and *A. sp. Kazakhstan* genomes to the new *A. sinica* assembly

We aligned the *A. sinica* published transcriptome (Huylmans *et al.* 2021) to both the *A. franciscana* and to the *A. sp Kazakhstan* genomic scaffolds using blat (Standalone BLAT v. 36x2, Kent 2002). For each transcript, we kept only the mapping location with the highest score in each genome (using the customized script 1-besthitblat.pl). When multiple transcripts overlapped by more than 20bps on the genome, only the transcript with the highest mapping score was kept (2-redremov_blat_v2.pl). We then used the location of the transcripts on the *Artemia sinica* genome to infer the location of the *A. franciscana* and *A. sp. Kazakhstan* scaffolds based on the transcripts they carried (AssignScaffoldLocation.pl). This script uses a majority rule to assign each scaffold to a chromosome, and then the mean location of genes on that scaffold to infer its final coordinate on the chromosome. All scripts are available on our Git page.

FST between male and female populations

RNA-seq reads from 10 pooled *A. sinica* males and 10 pooled *A. sinica* females (from Huylmans et al, 2021), sampled from head, thorax and gonads, were pooled by sex and mapped separately to the male *A.sinica* reference genome using STAR (Dobin *et al.* 2013) with default parameters.

bioRxiv preprint doi: https://doi.org/10.1101/2022.04.27.489735; this version posted April 29, 2022. The copyright holder for this preprint (which was not certified by peer review) is the author/funder, who has granted bioRxiv a license to display the preprint in perpetuity. It is made available under aCC-BY 4.0 International license.

The resulting alignments with MAPQ score lower than 20 were filtered out and the remaining alignments were sorted using samtools view and sort functions (Li *et al.* 2009). Next, a pileup file of male and female alignments was produced using samtools-mpileup function. Finally, we used scripts from the Popoolation2 package (Kofler *et al.* 2011) to calculate FST. The mpileup file was reformatted with the Popoolation2 mpileup2sync.pl script, and the resulting synchronized file was used as an input for fst-sliding.pl script. FST between male and female populations was calculated for windows of 1000 nucleotides, using the fst-sliding.pl script with following options --suppress-noninformative --min-count 3 --min-coverage 10 --max-coverage 200 --min-covered-fraction 0.5 --window-size 1000 --step-size 1000 --pool-size 10.

Identification of candidate W-genes with Kmer analysis:

We used a k-mer based subtraction approach (Elkrewi et al., 2021) based on the BBMap package (Bushnell, 2014) on male and female genomic and RNA-seq data from *A. franciscana* and *A. sinica*. The pipeline was applied to each species separately. In *A. sinica,* two male and two female DNA libraries and two whole body RNA-seq replicates for each sex were used (Sup. Tables 3 and 4). In *A. franciscana*, the analysis was performed using one male and one female DNA libraries and pools of two RNA-seq replicates of heads and gonads for each sex, along with one whole body male and female RNA-seq libraries (SRR14598203 and SRR14598204).

First, the shared 31-mers between the female DNA and RNA libraries were identified, and then any k-mers matching male libraries were removed. Female RNA-seq reads containing these female-specific Kmers [with minimum kmer fraction of 0.6 (mkf=0.6)] were retrieved and assembled using Trinity (Grabherr *et al.* 2011), and the perl script from the Trinity package (get_longest_isoform_seq_per_trinity_gene.pl) was used to keep only the longest isoform. The male and female genomic libraries were mapped to the assembled transcripts using Bowtie2 (Langmead and Salzberg 2012 p. 2), and candidates with a sum of female perfect matches <=8

bioRxiv preprint doi: https://doi.org/10.1101/2022.04.27.489735; this version posted April 29, 2022. The copyright holder for this preprint (which was not certified by peer review) is the author/funder, who has granted bioRxiv a license to display the preprint in perpetuity. It is made available under aCC-BY 4.0 International license.

and a ratio of sum-of-females/sum-of-males <=2 were removed. The final set consisted of 402 transcripts in *A. franciscana* and 319 in *A. sinica*.

Mapping of W candidates to the *A. sinica* genome

The *A. sinica* and *A. franciscana* W candidates were mapped to the *A. sinica* genome assembly with Parallel Blat (Wang and Kong 2019) with a translated query and database, and a minimum match score of 50. Only the mapping location with the strongest match score was considered for each transcript.

Transcriptome assemblies and expression analysis:

The *A. sinica* male transcriptome was assembled from two replicates of male whole body RNA-seq data (Huylmans *et al.* 2021) using Trinity (Grabherr *et al.* 2011) in two different modes: denovo and genome-guided. The two assemblies were concatenated and then filtered using the tr2aacds.pl script from EvidentialGene (Gilbert 2019). For the expression analysis, only the first isoform was kept for each gene, and only transcripts longer than 500bp were used in the analysis. The RNA-seq reads from the *A. sinica* heads, gonads, and thoraces of males and females (Huylmans *et al.* 2021) were mapped to the curated transcriptome and TPM values were obtained using Kallisto v.0.46.2, (Bray *et al.* 2016). Normalization was done using NormalyzerDE (Willforss *et al.* 2019).

Two different *A. franciscana* de novo transcriptome assemblies were made using Trinity. The first using pooled RNA-seq reads from male heads and testes (two replicates each, Huylmans *et al.* 2019), and the second using the published whole-body male RNA-seq library (SRR14598203, Jo *et al.* 2021b). The two assemblies were concatenated and then filtered using the tr2aacds.pl script from EvidentialGene.

bioRxiv preprint doi: https://doi.org/10.1101/2022.04.27.489735; this version posted April 29, 2022. The copyright holder for this preprint (which was not certified by peer review) is the author/funder, who has granted bioRxiv a license to display the preprint in perpetuity. It is made available under aCC-BY 4.0 International license.

559 **Phylogenetic Trees**

560 The W candidates of *A. sinica* and *A. franciscana* were mapped reciprocally to each other
561 using pblat (BLAT with parallel supports v. 36x2 with default parameters, Wang and Kong
562 2019), and reciprocal best hits were considered shared candidates. The W candidates of the
563 two species were further mapped to their respective uncollapsed male transcriptome
564 assemblies (see previous section) with pblat (Wang and Kong 2019) with a translated query and
565 database, and a minimum match score of 50. The transcripts with the highest mapping score to
566 the W candidates were used as the putative Z homologs in their respective species.

567 The *Branchinecta lindahli* transcriptome (Schwentner *et al.* 2018) was downloaded from the
568 Crustacean Phylogeny dataset on Harvard Dataverse (https://doi.org/10.7910/DVN/SM7DIU). *B.*
569 *lindahli* homologs of shared W-candidates were obtained by mapping the putative Z homologs
570 of both species to the *B. lindahli* transcriptome using pblat (-minScore=50 -t=dnax -q=dnax) and
571 retrieving the transcript with highest alignments score (using the customized script 2-
572 besthitblat.pl). A transcript was considered a homolog if it mapped to at least one of the putative
573 Z homologs of the two species, and when the two Z homologs mapped to different outgroup
574 sequences, both outgroup sequences were retrieved and used to make two different
575 alignments.

576 The shared W candidates of *A. sinica* and *A. franciscana*, their Z homologs, and the
577 outgroup sequences were aligned using MAFFT (v7.487, with the options “mafft --
578 adjustdirection INPUT > OUTPUT”, Katoh *et al.* 2002). The resulting alignments were fed to
579 phylogeny.fr (Dereeper *et al.* 2008), where the alignment was curated using GBLOCKS
580 (Talavera and Castresana 2007), and the phylogenetic tree was constructed using PhyML
581 (Guindon *et al.* 2010). Trees were made only for sequences where the number of overlapping
582 positions after gblocks was longer than 200bp (Sup. Fig. 7). In the four instances where the
583 curated alignment length with the outgroup was shorter than 200bp, we tried aligning the
584 sequences without the outgroup. For the two cases where the resulting alignment length was

bioRxiv preprint doi: https://doi.org/10.1101/2022.04.27.489735; this version posted April 29, 2022. The copyright holder for this preprint (which was not certified by peer review) is the author/funder, who has granted bioRxiv a license to display the preprint in perpetuity. It is made available under aCC-BY 4.0 International license.

longer than or equal 200bp, unrooted trees were made (Sup. Fig. 7). The trees were then downloaded in the Newick format and visualized using itol.embl.de (Letunic and Bork 2019).

Heterozygosity analysis in asexual female and rare male

Illumina genomic sequencing was performed on a rare male and its asexual sister (both derived from an Aibi Lake *A. parthenogenetica* lineage), yielding around 115 million paired-end reads with a length of 125 nucleotides for each sample. The reads were quality- and adapter-trimmed with Trimmomatic-0.36 (Bolger *et al.* 2014), and mapped to the draft *Artemia sp. Kazakhstan* genome assembly using STAR v.2.6.0c (Dobin *et al.* 2013) with default settings.

We indexed the reference *A. sp. Kazakhstan* genome using SAMtools v.1.10 (Li *et al.* 2009), called the SNPs from BAM alignments with BCFtools v.1.10.2 (Li *et al.* 2009), then removed indels, filtered for quality of reads over 30 and coverage over 5 and below 100 with VCFtools v.0.1.15 (Danecek *et al.* 2011), and removed multiallelic sites with BCFtools.

We calculated the fraction of SNPs that lost heterozygosity in the rare male DNA in comparison with the asexual sister DNA. It was calculated and visualized in 500kb bins for each chromosome.

Analysis of backcross between the Aibi Lake rare male and *A. sp. Kazakhstan* females

We sequenced 5 asexual females and 10 putatively sexual females from the F2 generation. This resulted in an average of 101 million reads per asexual female and 50 million reads per putatively sexual female. We removed adaptors and trimmed reads using Trimmomatic v0.39 (Bolger *et al.* 2014). We then aligned the resulting paired-end reads to the genome using Bowtie2 v2.4.4 (Langmead and Salzberg 2012). SAM files were converted to BAM files and sorted in Samtools v.1.13 (Li *et al.* 2009).

For our pooled analyses, we merged BAM files into a pooled asexual BAM file and a pooled putatively-sexual BAM, and created a mpileup file in Samtools v.1.13. We then used

bioRxiv preprint doi: https://doi.org/10.1101/2022.04.27.489735; this version posted April 29, 2022. The copyright holder for this preprint (which was not certified by peer review) is the author/funder, who has granted bioRxiv a license to display the preprint in perpetuity. It is made available under aCC-BY 4.0 International license.

611 Popoolation2 (Kofler *et al.* 2011) to call FST for both individual SNPs and in 1kb windows. We
612 used FST computed for 1kb windows to visualize FST across the genome in a Manhattan plot in
613 the R package qqman (Turner 2018). We computed rolling medians in sliding windows of 101
614 consecutive SNPs on each linkage group using the rollmedian function from the package zoo
615 (Zeileis and Grothendieck 2005) in R v.4.0.3. To identify regions of elevated FST on individual
616 chromosomes, we computed 95% confidence intervals by sampling rolling medians of 101
617 consecutive SNPs across the genome 1000 times.

618 For our individual-based analyses, we first used SEQTK v1.2 (https://github.com/lh3/seqtk)
619 to randomly select a subset of reads from each asexual sample to match the highest coverage
620 found in an F2 control female (to avoid biases caused by the much larger number of reads
621 obtained for the F2 asexuals than for the controls). We then mapped reads from all F2
622 individuals to the *A. sp. Kazakhstan* genome using BWA mem v0.7.17 (Li and Durbin 2009) with
623 default parameters. DNA reads from the rare male and its *A. parthenogenetica* sister, and from
624 two *A. sp. Kazakhstan* individuals, were also subsetted and mapped. The resulting BAM
625 alignments were sorted with samtools v1.14 (Li *et al.* 2009), and used to call SNPs with the
626 mpileup function of BCFtools v1.14 (Li 2011). The VCF file was filtered with VCFtools v0.1.17
627 (Danecek *et al.* 2011) for minimum and maximum depth (4 and 50), minimum quality score (30)
628 and minimum minor allele frequency (0.1). Only SNPs for which the two *A. sp. Kazakhstan* had
629 a genotype of 0/0, and the two *A. parthenogenetica* individuals 1/1, were kept for further
630 analyses. We computed FST between the F2 asexual and control females using the function --
631 weir-fst-pop in VCFtools for 10kb windows. We then inferred ancestry of each genomic scaffold
632 in every sample (i.e. whether they were homozygous for the *A. sp. Kazakhstan* haplotype, or
633 carried a copy of the *A. parthenogenetica* haplotype as well) using the customized script
634 Chromopaint.pl (available on our git page). The *A. sp. Kazakhstan* genomic scaffolds were
635 assigned to a location on the *A. sinica* genome as before. Scaffolds with more than 10
636 informative SNPs, and >80% 0/1 or 1/1 SNPs were considered to be heterozygous for the *A.*

bioRxiv preprint doi: https://doi.org/10.1101/2022.04.27.489735; this version posted April 29, 2022. The copyright holder for this preprint (which was not certified by peer review) is the author/funder, who has granted bioRxiv a license to display the preprint in perpetuity. It is made available under aCC-BY 4.0 International license.

637 *sp. Kazakhstan* and *A. parthenogenetica* haplotypes, whereas scaffolds with >80% 0/0 were
638 considered to have only *A. sp. Kazakhstan* ancestry (only 5 to 9% of scaffolds fell in between
639 and could not be classified in each individual).
640
641 **Acknowledgements**
642 We thank the Vicoso group for comments on the manuscript, and the ISTA Scientific computing
643 team and the Vienna Biocenter Sequencing facility for technical support. This work was
644 supported by the European Research Council under the European Union's Horizon 2020
645 research and innovation program (grant agreement no. 715257).
646
647 **Reference**
648 Abatzopoulos T. J., 2018 The repeated emergence of asexuality, the hidden genomes and the
649 role of parthenogenetic rare males in the brine shrimp Artemia. J. Biol. Res.-Thessalon.
650 25: 7. https://doi.org/10.1186/s40709-018-0078-2
651 Accioly I. V., I. M. C. da Cunha, J. C. M. Tavares, and W. F. Molina, 2015 CHROMOSOME
652 BANDING IN CRUSTACEA. I. KARYOTYPE, Ag-NORs, C BANDING AND
653 TREATMENT WITH EcoRI, PstI and KpnI RESTRICTION ENDONUCLEASES IN
654 Artemia franciscana. Biota Amaz. Biote Amaz. Biota Amazon. Amaz. Biota.
655 Argyridou E., and J. Parsch, 2018 Regulation of the X Chromosome in the Germline and Soma
656 of Drosophila melanogaster Males. Genes 9: 242. https://doi.org/10.3390/genes9050242
657 Arima Genomics, 2021 *mapping_pipeline*. Arima Genomics, Inc.
658 Aumer D., M. H. Allsopp, H. M. G. Lattorff, R. F. A. Moritz, and A. Jarosch-Perlow, 2017
659 Thelytoky in Cape honeybees (Apis mellifera capensis) is controlled by a single
660 recessive locus
661 Bachtrog D., 2013 Y-chromosome evolution: emerging insights into processes of Y-
662 chromosome degeneration. Nat. Rev. Genet. 14: 113–124.

bioRxiv preprint doi: https://doi.org/10.1101/2022.04.27.489735; this version posted April 29, 2022. The copyright holder for this preprint (which was not certified by peer review) is the author/funder, who has granted bioRxiv a license to display the preprint in perpetuity. It is made available under aCC-BY 4.0 International license.

https://doi.org/10.1038/nrg3366

Bachtrog D., J. E. Mank, C. L. Peichel, M. Kirkpatrick, S. P. Otto, *et al.*, 2014 Sex Determination: Why So Many Ways of Doing It? PLOS Biol. 12: e1001899. https://doi.org/10.1371/journal.pbio.1001899

Baxevanis A. D., I. Kappas, and T. J. Abatzopoulos, 2006 Molecular phylogenetics and asexuality in the brine shrimp Artemia. Mol. Phylogenet. Evol. 40: 724–738. https://doi.org/10.1016/j.ympev.2006.04.010

Beukeboom L. W., and N. Perrin, 2014 *The Evolution of Sex Determination*. Oxford University Press, Oxford.

Bolger A. M., M. Lohse, and B. Usadel, 2014 Trimmomatic: a flexible trimmer for Illumina sequence data. Bioinformatics 30: 2114–2120. https://doi.org/10.1093/bioinformatics/btu170

Bowen S. T., 1963 The Genetics of Artemia salina. III. Effects of X-Irradiation and of Freezing upon Cysts. Biol. Bull. 125: 431–440. https://doi.org/10.2307/1539357

Boyer L., R. Jabbour□Zahab, M. Mosna, C. R. Haag, and T. Lenormand, 2021 Not so clonal asexuals: Unraveling the secret sex life of Artemia parthenogenetica. Evol. Lett. 5: 164–174. https://doi.org/10.1002/evl3.216

Boyer L., R. Jabbour-Zahab, P. Joncour, S. Glémin, C. R. Haag, *et al.*, 2022 Asexual male production by ZW recombination in Artemia parthenogenetica. 2022.04.01.486774.

Bray N. L., H. Pimentel, P. Melsted, and L. Pachter, 2016 Near-optimal probabilistic RNA-seq quantification. Nat. Biotechnol. 34: 525–527. https://doi.org/10.1038/nbt.3519

Bushnell B., 2014 BBMap: A Fast, Accurate, Splice-Aware Aligner

Chakraborty M., J. G. Baldwin-Brown, A. D. Long, and J. J. Emerson, 2016 Contiguous and accurate de novo assembly of metazoan genomes with modest long read coverage. Nucleic Acids Res. 44: e147. https://doi.org/10.1093/nar/gkw654

Chan W., A. E. P. Shaughnessy, C. P. van den Berg, M. J. Garson, and K. L. Cheney, 2021 The

bioRxiv preprint doi: https://doi.org/10.1101/2022.04.27.489735; this version posted April 29, 2022. The copyright holder for this preprint (which was not certified by peer review) is the author/funder, who has granted bioRxiv a license to display the preprint in perpetuity. It is made available under aCC-BY 4.0 International license.

689 Validity of Brine Shrimp (Artemia Sp.) Toxicity Assays to Assess the Ecological Function
690 of Marine Natural Products. J. Chem. Ecol. 47: 834–846. https://doi.org/10.1007/s10886-
691 021-01264-z
692 Charlesworth B., 1978 Model for evolution of Y chromosomes and dosage compensation. Proc.
693 Natl. Acad. Sci. 75: 5618–5622. https://doi.org/10.1073/pnas.75.11.5618
694 Charlesworth D., B. Charlesworth, and G. Marais, 2005 Steps in the evolution of heteromorphic
695 sex chromosomes. Heredity 95: 118–128. https://doi.org/10.1038/sj.hdy.6800697
696 Charlesworth D., 2019 Young sex chromosomes in plants and animals. New Phytol. 224: 1095–
697 1107. https://doi.org/10.1111/nph.16002
698 Danecek P., A. Auton, G. Abecasis, C. A. Albers, E. Banks, *et al.*, 2011 The variant call format
699 and VCFtools. Bioinformatics 27: 2156–2158.
700 https://doi.org/10.1093/bioinformatics/btr330
701 De Vos S., P. Bossier, G. Van Stappen, I. Vercauteren, P. Sorgeloos, *et al.*, 2013 A first AFLP-
702 based genetic linkage map for brine shrimp Artemia franciscana and its application in
703 mapping the sex locus. PloS One 8: e57585.
704 https://doi.org/10.1371/journal.pone.0057585
705 De Vos S., S. Rombauts, L. Coussement, W. Dermauw, M. Vuylsteke, *et al.*, 2021 The genome
706 of the extremophile Artemia provides insight into strategies to cope with extreme
707 environments. BMC Genomics 22: 635. https://doi.org/10.1186/s12864-021-07937-z
708 Dereeper A., V. Guignon, G. Blanc, S. Audic, S. Buffet, *et al.*, 2008 Phylogeny.fr: robust
709 phylogenetic analysis for the non-specialist. Nucleic Acids Res. 36: W465–W469.
710 https://doi.org/10.1093/nar/gkn180
711 Disteche C. M., 2016 Dosage compensation of the sex chromosomes and autosomes. Semin.
712 Cell Dev. Biol. 56: 9–18. https://doi.org/10.1016/j.semcdb.2016.04.013
713 Dobin A., C. A. Davis, F. Schlesinger, J. Drenkow, C. Zaleski, *et al.*, 2013 STAR: ultrafast
714 universal RNA-seq aligner. Bioinformatics 29: 15–21.

bioRxiv preprint doi: https://doi.org/10.1101/2022.04.27.489735; this version posted April 29, 2022. The copyright holder for this preprint (which was not certified by peer review) is the author/funder, who has granted bioRxiv a license to display the preprint in perpetuity. It is made available under aCC-BY 4.0 International license.

https://doi.org/10.1093/bioinformatics/bts635

Eads B. D., D. Tsuchiya, J. Andrews, M. Lynch, and M. E. Zolan, 2012 The spread of a transposon insertion in Rec8 is associated with obligate asexuality in Daphnia. Proc. Natl. Acad. Sci. 109: 858–863. https://doi.org/10.1073/pnas.1119667109

Elkrewi M., M. A. Moldovan, M. A. L. Picard, and B. Vicoso, 2021 Schistosome W-Linked Genes Inform Temporal Dynamics of Sex Chromosome Evolution and Suggest Candidate for Sex Determination. Mol. Biol. Evol. 38: 5345–5358. https://doi.org/10.1093/molbev/msab178

Ellegren H., 2011 Sex-chromosome evolution: recent progress and the influence of male and female heterogamety. Nat. Rev. Genet. 12: 157–166. https://doi.org/10.1038/nrg2948

Gajardo G., and J. Beardmore, 2012 The Brine Shrimp Artemia: Adapted to Critical Life Conditions. Front. Physiol. 3.

Gammerdinger W. J., M. A. Toups, and B. Vicoso, 2020 Disagreement in F ST estimators: A case study from sex chromosomes. Mol. Ecol. Resour. 20: 1517–1525. https://doi.org/10.1111/1755-0998.13210

Gilbert D. G., 2019 Longest protein, longest transcript or most expression, for accurate gene reconstruction of transcriptomes? 829184.

Grabherr M. G., B. J. Haas, M. Yassour, J. Z. Levin, D. A. Thompson, *et al.*, 2011 Trinity: reconstructing a full-length transcriptome without a genome from RNA-Seq data. Nat. Biotechnol. 29: 644–652. https://doi.org/10.1038/nbt.1883

Guan D., S. A. McCarthy, J. Wood, K. Howe, Y. Wang, *et al.*, 2020 Identifying and removing haplotypic duplication in primary genome assemblies. Bioinformatics 36: 2896–2898. https://doi.org/10.1093/bioinformatics/btaa025

Guindon S., J.-F. Dufayard, V. Lefort, M. Anisimova, W. Hordijk, *et al.*, 2010 New algorithms and methods to estimate maximum-likelihood phylogenies: assessing the performance of PhyML 3.0. Syst. Biol. 59: 307–321. https://doi.org/10.1093/sysbio/syq010

bioRxiv preprint doi: https://doi.org/10.1101/2022.04.27.489735; this version posted April 29, 2022. The copyright holder for this preprint (which was not certified by peer review) is the author/funder, who has granted bioRxiv a license to display the preprint in perpetuity. It is made available under aCC-BY 4.0 International license.

741 Haag C. R., L. Theodosiou, R. Zahab, and T. Lenormand, 2017 Low recombination rates in
742 sexual species and sex–asex transitions. Philos. Trans. R. Soc. B Biol. Sci. 372:
743 20160461. https://doi.org/10.1098/rstb.2016.0461
744 Han X., Y. Ren, X. Ouyang, B. Zhang, and L. Sui, 2021 Construction of a high-density genetic
745 linkage map and QTL mapping for sex and growth traits in Artemia franciscana.
746 Aquaculture 540: 736692. https://doi.org/10.1016/j.aquaculture.2021.736692
747 Handley L.-J. L., H. Ceplitis, and H. Ellegren, 2004 Evolutionary strata on the chicken Z
748 chromosome: implications for sex chromosome evolution. Genetics 167: 367–376.
749 Huylmans A. K., A. Macon, and B. Vicoso, 2017 Global Dosage Compensation Is Ubiquitous in
750 Lepidoptera, but Counteracted by the Masculinization of the Z Chromosome. Mol. Biol.
751 Evol. 34: 2637–2649. https://doi.org/10.1093/molbev/msx190
752 Huylmans A. K., M. A. Toups, A. Macon, W. J. Gammerdinger, and B. Vicoso, 2019 Sex-Biased
753 Gene Expression and Dosage Compensation on the Artemia franciscana Z-
754 Chromosome. Genome Biol. Evol. 11: 1033–1044. https://doi.org/10.1093/gbe/evz053
755 Huylmans A. K., A. Macon, F. Hontoria, and B. Vicoso, 2021 Transitions to asexuality and
756 evolution of gene expression in Artemia brine shrimp. Proc. Biol. Sci. 288: 20211720.
757 https://doi.org/10.1098/rspb.2021.1720
758 Jaquiéry J., S. Stoeckel, C. Larose, P. Nouhaud, C. Rispe, *et al.*, 2014 Genetic Control of
759 Contagious Asexuality in the Pea Aphid. PLOS Genet. 10: e1004838.
760 https://doi.org/10.1371/journal.pgen.1004838
761 Jo E., S. J. Lee, E. Choi, J. Kim, S. G. Lee, *et al.*, 2021a Whole genome survey and
762 microsatellite motif identification of Artemia franciscana. Biosci. Rep. 41: BSR20203868.
763 https://doi.org/10.1042/BSR20203868
764 Jo E., S.-J. Lee, E. Choi, J. Kim, J.-H. Lee, *et al.*, 2021b Sex-Biased Gene Expression and
765 Isoform Profile of Brine Shrimp Artemia franciscana by Transcriptome Analysis. Anim.
766 Open Access J. MDPI 11: 2630. https://doi.org/10.3390/ani11092630

bioRxiv preprint doi: https://doi.org/10.1101/2022.04.27.489735; this version posted April 29, 2022. The copyright holder for this preprint (which was not certified by peer review) is the author/funder, who has granted bioRxiv a license to display the preprint in perpetuity. It is made available under aCC-BY 4.0 International license.

767 Kampfraath A. A., T. P. Dudink, K. Kraaijeveld, J. Ellers, and Z. V. Zizzari, 2020 Male Sexual
768 Trait Decay in Two Asexual Springtail Populations Follows Neutral Mutation
769 Accumulation Theory. Evol. Biol. 47: 285–292. https://doi.org/10.1007/s11692-020-
770 09511-z
771 Katoh K., K. Misawa, K. Kuma, and T. Miyata, 2002 MAFFT: a novel method for rapid multiple
772 sequence alignment based on fast Fourier transform. Nucleic Acids Res. 30: 3059–
773 3066. https://doi.org/10.1093/nar/gkf436
774 Katsuma S., K. Shoji, Y. Sugano, Y. Suzuki, and T. Kiuchi, 2019 Masc-induced dosage
775 compensation in silkworm cultured cells. FEBS Open Bio 9: 1573–1579.
776 https://doi.org/10.1002/2211-5463.12698
777 Kent W. J., 2002 BLAT--the BLAST-like alignment tool. Genome Res. 12: 656–664.
778 https://doi.org/10.1101/gr.229202
779 Kiuchi T., H. Koga, M. Kawamoto, K. Shoji, H. Sakai, *et al.*, 2014 A single female-specific piRNA
780 is the primary determiner of sex in the silkworm. Nature 509: 633–636.
781 https://doi.org/10.1038/nature13315
782 Kofler R., R. V. Pandey, and C. Schlötterer, 2011 PoPoolation2: identifying differentiation
783 between populations using sequencing of pooled DNA samples (Pool-Seq).
784 Bioinformatics 27: 3435–3436. https://doi.org/10.1093/bioinformatics/btr589
785 Kolmogorov M., J. Yuan, Y. Lin, and P. A. Pevzner, 2019 Assembly of long, error-prone reads
786 using repeat graphs. Nat. Biotechnol. 37: 540–546. https://doi.org/10.1038/s41587-019-
787 0072-8
788 Lahn B. T., and D. C. Page, 1999 Four evolutionary strata on the human X chromosome.
789 Science 286: 964–967. https://doi.org/10.1126/science.286.5441.964
790 Langmead B., and S. L. Salzberg, 2012 Fast gapped-read alignment with Bowtie 2. Nat.
791 Methods 9: 357–359. https://doi.org/10.1038/nmeth.1923
792 Letunic I., and P. Bork, 2019 Interactive Tree Of Life (iTOL) v4: recent updates and new

bioRxiv preprint doi: https://doi.org/10.1101/2022.04.27.489735; this version posted April 29, 2022. The copyright holder for this preprint (which was not certified by peer review) is the author/funder, who has granted bioRxiv a license to display the preprint in perpetuity. It is made available under aCC-BY 4.0 International license.

793 developments. Nucleic Acids Res. 47: W256–W259. https://doi.org/10.1093/nar/gkz239

794 Li H., and R. Durbin, 2009 Fast and accurate short read alignment with Burrows-Wheeler

795 transform. Bioinforma. Oxf. Engl. 25: 1754–1760.

796 https://doi.org/10.1093/bioinformatics/btp324

797 Li H., B. Handsaker, A. Wysoker, T. Fennell, J. Ruan, *et al.*, 2009 The Sequence

798 Alignment/Map format and SAMtools. Bioinformatics 25: 2078–2079.

799 https://doi.org/10.1093/bioinformatics/btp352

800 Li H., 2011 A statistical framework for SNP calling, mutation discovery, association mapping and

801 population genetical parameter estimation from sequencing data. Bioinformatics 27:

802 2987–2993. https://doi.org/10.1093/bioinformatics/btr509

803 Li D., C.-M. Liu, R. Luo, K. Sadakane, and T.-W. Lam, 2015 MEGAHIT: an ultra-fast single-node

804 solution for large and complex metagenomics assembly via succinct de Bruijn graph.

805 Bioinformatics 31: 1674–1676. https://doi.org/10.1093/bioinformatics/btv033

806 Li H., 2016 Minimap and miniasm: fast mapping and de novo assembly for noisy long

807 sequences. Bioinformatics 32: 2103–2110. https://doi.org/10.1093/bioinformatics/btw152

808 Luo R., B. Liu, Y. Xie, Z. Li, W. Huang, *et al.*, 2012 SOAPdenovo2: an empirically improved

809 memory-efficient short-read de novo assembler. GigaScience 1: 2047-217X-1–18.

810 https://doi.org/10.1186/2047-217X-1-18

811 Lynch M., A. Seyfert, B. Eads, and E. Williams, 2008 Localization of the Genetic Determinants

812 of Meiosis Suppression in Daphnia pulex. Genetics 180: 317–327.

813 https://doi.org/10.1534/genetics.107.084657

814 Maccari M., A. Gómez, F. Hontoria, and F. Amat, 2013a Functional rare males in diploid

815 parthenogenetic Artemia. J. Evol. Biol. 26: 1934–1948. https://doi.org/10.1111/jeb.12191

816 Maccari M., F. Amat, and A. Gómez, 2013b Origin and Genetic Diversity of Diploid

817 Parthenogenetic Artemia in Eurasia. PLOS ONE 8: e83348.

818 https://doi.org/10.1371/journal.pone.0083348

bioRxiv preprint doi: https://doi.org/10.1101/2022.04.27.489735; this version posted April 29, 2022. The copyright holder for this preprint (which was not certified by peer review) is the author/funder, who has granted bioRxiv a license to display the preprint in perpetuity. It is made available under aCC-BY 4.0 International license.

819 Maccari M., F. Amat, F. Hontoria, and A. Gómez, 2014 Laboratory generation of new
820 parthenogenetic lineages supports contagious parthenogenesis in Artemia. PeerJ 2:
821 e439. https://doi.org/10.7717/peerj.439
822 MacRae T. H., 2003 Molecular chaperones, stress resistance and development in Artemia
823 franciscana. Semin. Cell Dev. Biol. 14: 251–258.
824 https://doi.org/10.1016/j.semcdb.2003.09.019
825 Mank J. E., 2013 Sex chromosome dosage compensation: definitely not for everyone. Trends
826 Genet. 29: 677–683. https://doi.org/10.1016/j.tig.2013.07.005
827 Manni M., M. R. Berkeley, M. Seppey, F. A. Simão, and E. M. Zdobnov, 2021 BUSCO Update:
828 Novel and Streamlined Workflows along with Broader and Deeper Phylogenetic
829 Coverage for Scoring of Eukaryotic, Prokaryotic, and Viral Genomes. Mol. Biol. Evol. 38:
830 4647–4654. https://doi.org/10.1093/molbev/msab199
831 Meiklejohn C. D., E. L. Landeen, J. M. Cook, S. B. Kingan, and D. C. Presgraves, 2011 Sex
832 chromosome-specific regulation in the Drosophila male germline but little evidence for
833 chromosomal dosage compensation or meiotic inactivation. PLoS Biol. 9: e1001126.
834 https://doi.org/10.1371/journal.pbio.1001126
835 Mignerot L., K. Avia, R. Luthringer, A. P. Lipinska, A. F. Peters, *et al.*, 2019 A key role for sex
836 chromosomes in the regulation of parthenogenesis in the brown alga Ectocarpus. PLoS
837 Genet. 15: e1008211. https://doi.org/10.1371/journal.pgen.1008211
838 Mullon C., A. E. Wright, M. Reuter, A. Pomiankowski, and J. E. Mank, 2015 Evolution of dosage
839 compensation under sexual selection differs between X and Z chromosomes. Nat.
840 Commun. 6: 7720. https://doi.org/10.1038/ncomms8720
841 Neiman M., T. F. Sharbel, and T. Schwander, 2014 Genetic causes of transitions from sexual
842 reproduction to asexuality in plants and animals. J. Evol. Biol. 27: 1346–1359.
843 https://doi.org/10.1111/jeb.12357
844 Nougué O., N. O. Rode, R. Jabbour-Zahab, A. Ségard, L.-M. Chevin, *et al.*, 2015 Automixis in

bioRxiv preprint doi: https://doi.org/10.1101/2022.04.27.489735; this version posted April 29, 2022. The copyright holder for this preprint (which was not certified by peer review) is the author/funder, who has granted bioRxiv a license to display the preprint in perpetuity. It is made available under aCC-BY 4.0 International license.

Artemia: solving a century-old controversy. J. Evol. Biol. 28: 2337–2348. https://doi.org/10.1111/jeb.12757

Ntungwe N E., E. M. Domínguez-Martín, A. Roberto, J. Tavares, V. M. S. Isca, *et al.*, 2020 Artemia species: An Important Tool to Screen General Toxicity Samples. Curr. Pharm. Des. 26: 2892–2908. https://doi.org/10.2174/1381612826666200406083035

Okumu M. O., J. M. Mbaria, J. K. Gikunju, P. G. Mbuthia, V. O. Madadi, *et al.*, 2021 Artemia salina as an animal model for the preliminary evaluation of snake venom-induced toxicity. Toxicon X 12: 100082. https://doi.org/10.1016/j.toxcx.2021.100082

Palmer D. H., T. F. Rogers, R. Dean, and A. E. Wright, 2019 How to identify sex chromosomes and their turnover. Mol. Ecol. 28: 4709–4724. https://doi.org/10.1111/mec.15245

Parraguez M., G. Gajardo, and J. A. Beardmore, 2009 The New World Artemia species A. franciscana and A. persimilis are highly differentiated for chromosome size and heterochromatin content. Hereditas 146: 93–103. https://doi.org/10.1111/j.1601-5223.2009.02109.x

Pennell M. W., J. E. Mank, and C. L. Peichel, 2018 Transitions in sex determination and sex chromosomes across vertebrate species. Mol. Ecol. 27: 3950–3963. https://doi.org/10.1111/mec.14540

Picard M. A. L., C. Cosseau, S. Ferré, T. Quack, C. G. Grevelding, *et al.*, 2018 Evolution of gene dosage on the Z-chromosome of schistosome parasites. eLife 7: e35684. https://doi.org/10.7554/eLife.35684

Picard M. A. L., B. Vicoso, S. Bertrand, and H. Escriva, 2021 Diversity of Modes of Reproduction and Sex Determination Systems in Invertebrates, and the Putative Contribution of Genetic Conflict. Genes 12: 1136. https://doi.org/10.3390/genes12081136

Ponnikas S., H. Sigeman, J. K. Abbott, and B. Hansson, 2018 Why Do Sex Chromosomes Stop Recombining? Trends Genet. 34: 492–503. https://doi.org/10.1016/j.tig.2018.04.001

bioRxiv preprint doi: https://doi.org/10.1101/2022.04.27.489735; this version posted April 29, 2022. The copyright holder for this preprint (which was not certified by peer review) is the author/funder, who has granted bioRxiv a license to display the preprint in perpetuity. It is made available under aCC-BY 4.0 International license.

871 Rajabi S., A. Ramazani, M. Hamidi, and T. Naji, 2015 Artemia salina as a model organism in
872 toxicity assessment of nanoparticles. DARU J. Pharm. Sci. 23: 20.
873 https://doi.org/10.1186/s40199-015-0105-x
874 Robinson J. T., D. Turner, N. C. Durand, H. Thorvaldsdóttir, J. P. Mesirov, *et al.*, 2018
875 Juicebox.js Provides a Cloud-Based Visualization System for Hi-C Data. Cell Syst. 6:
876 256-258.e1. https://doi.org/10.1016/j.cels.2018.01.001
877 Rode N. O., R. Jabbour-Zahab, L. Boyer, É. Flaven, F. Hontoria, *et al.*, 2021 The origin of
878 asexual brine shrimps. 2021.06.11.448048.
879 Rosin L. F., D. Chen, Y. Chen, and E. P. Lei, 2022 Dosage compensation in Bombyx mori is
880 achieved by partial repression of both Z chromosomes in males. Proc. Natl. Acad. Sci.
881 119: e2113374119. https://doi.org/10.1073/pnas.2113374119
882 Rovatsos M., and L. Kratochvíl, 2021 Evolution of dosage compensation does not depend on
883 genomic background. Mol. Ecol. 30: 1836–1845. https://doi.org/10.1111/mec.15853
884 Ruan J., and H. Li, 2020 Fast and accurate long-read assembly with wtdbg2. Nat. Methods 17:
885 155–158. https://doi.org/10.1038/s41592-019-0669-3
886 Sainz-Escudero L., E. K. López-Estrada, P. C. Rodríguez-Flores, and M. García-París, 2021
887 Settling taxonomic and nomenclatural problems in brine shrimps, Artemia (Crustacea:
888 Branchiopoda: Anostraca), by integrating mitogenomics, marker discordances and
889 nomenclature rules. PeerJ 9: e10865. https://doi.org/10.7717/peerj.10865
890 Sandrock C., and C. Vorburger, 2011 Single-Locus Recessive Inheritance of Asexual
891 Reproduction in a Parasitoid Wasp. Curr. Biol. 21: 433–437.
892 https://doi.org/10.1016/j.cub.2011.01.070
893 Schwander T., and B. J. Crespi, 2009 Multiple direct transitions from sexual reproduction to
894 apomictic parthenogenesis in Timema stick insects. Evol. Int. J. Org. Evol. 63: 84–103.
895 https://doi.org/10.1111/j.1558-5646.2008.00524.x
896 Schwentner M., S. Richter, D. C. Rogers, and G. Giribet, 2018 Tetraconatan phylogeny with

bioRxiv preprint doi: https://doi.org/10.1101/2022.04.27.489735; this version posted April 29, 2022. The copyright holder for this preprint (which was not certified by peer review) is the author/funder, who has granted bioRxiv a license to display the preprint in perpetuity. It is made available under aCC-BY 4.0 International license.

special focus on Malacostraca and Branchiopoda: highlighting the strength of taxon-specific matrices in phylogenomics. Proc. Biol. Sci. 285: 20181524. https://doi.org/10.1098/rspb.2018.1524

Sigeman H., M. Strandh, E. Proux-Wéra, V. E. Kutschera, S. Ponnikas, *et al.*, 2021 Avian Neo-Sex Chromosomes Reveal Dynamics of Recombination Suppression and W Degeneration. Mol. Biol. Evol. 38: 5275–5291. https://doi.org/10.1093/molbev/msab277

Spooner B. S., L. DeBell, L. Hawkins, J. Metcalf, J. A. Guikema, *et al.*, 1992 Brine Shrimp Development in Space: Ground-Based Data to Shuttle Flight Results. Trans. Kans. Acad. Sci. 1903- 95: 87–92. https://doi.org/10.2307/3628023

Straub T., and P. B. Becker, 2007 Dosage compensation: the beginning and end of generalization. Nat. Rev. Genet. 8: 47–57. https://doi.org/10.1038/nrg2013

Talavera G., and J. Castresana, 2007 Improvement of Phylogenies after Removing Divergent and Ambiguously Aligned Blocks from Protein Sequence Alignments. Syst. Biol. 56: 564–577. https://doi.org/10.1080/10635150701472164

Toman J., and J. Flegr, 2018 General environmental heterogeneity as the explanation of sexuality? Comparative study shows that ancient asexual taxa are associated with both biotically and abiotically homogeneous environments. Ecol. Evol. 8: 973–991. https://doi.org/10.1002/ece3.3716

Turner S. D., 2018 qqman: an R package for visualizing GWAS results using Q-Q and manhattan plots. J. Open Source Softw. 3: 731. https://doi.org/10.21105/joss.00731

Van Stappen G., 2002 Zoogeography, pp. 171–224 in *Artemia: Basic and Applied Biology*, Biology of Aquatic Organisms. edited by Abatzopoulos Th. J., Beardmore J. A., Clegg J. S., Sorgeloos P. Springer Netherlands, Dordrecht.

Vaser R., I. Sović, N. Nagarajan, and M. Šikić, 2017 Fast and accurate de novo genome assembly from long uncorrected reads. Genome Res. 27: 737–746. https://doi.org/10.1101/gr.214270.116

bioRxiv preprint doi: https://doi.org/10.1101/2022.04.27.489735; this version posted April 29, 2022. The copyright holder for this preprint (which was not certified by peer review) is the author/funder, who has granted bioRxiv a license to display the preprint in perpetuity. It is made available under aCC-BY 4.0 International license.

923 Vibranovski M. D., H. F. Lopes, T. L. Karr, and M. Long, 2009 Stage-Specific Expression
924 Profiling of Drosophila Spermatogenesis Suggests that Meiotic Sex Chromosome
925 Inactivation Drives Genomic Relocation of Testis-Expressed Genes. PLOS Genet. 5:
926 e1000731. https://doi.org/10.1371/journal.pgen.1000731
927 Vicoso B., and D. Bachtrog, 2009 Progress and prospects toward our understanding of the
928 evolution of dosage compensation. Chromosome Res. 17: 585.
929 https://doi.org/10.1007/s10577-009-9053-y
930 Vicoso B., J. J. Emerson, Y. Zektser, S. Mahajan, and D. Bachtrog, 2013 Comparative sex
931 chromosome genomics in snakes: differentiation, evolutionary strata, and lack of global
932 dosage compensation. PLoS Biol. 11: e1001643.
933 https://doi.org/10.1371/journal.pbio.1001643
934 Vicoso B., 2019 Molecular and evolutionary dynamics of animal sex-chromosome turnover. Nat.
935 Ecol. Evol. 3: 1632–1641. https://doi.org/10.1038/s41559-019-1050-8
936 Walters J. R., and T. J. Hardcastle, 2011 Getting a full dose? Reconsidering sex chromosome
937 dosage compensation in the silkworm, Bombyx mori. Genome Biol. Evol. 3: 491–504.
938 https://doi.org/10.1093/gbe/evr036
939 Wang M., and L. Kong, 2019 pblat: a multithread blat algorithm speeding up aligning sequences
940 to genomes. BMC Bioinformatics 20: 28. https://doi.org/10.1186/s12859-019-2597-8
941 Willforss J., A. Chawade, and F. Levander, 2019 NormalyzerDE: Online Tool for Improved
942 Normalization of Omics Expression Data and High-Sensitivity Differential Expression
943 Analysis. J. Proteome Res. 18: 732–740. https://doi.org/10.1021/acs.jproteome.8b00523
944 Wright A. E., R. Dean, F. Zimmer, and J. E. Mank, 2016 How to make a sex chromosome. Nat.
945 Commun. 7: 12087. https://doi.org/10.1038/ncomms12087
946 Yagound B., K. A. Dogantzis, A. Zayed, J. Lim, P. Broekhuyse, *et al.*, 2020 A Single Gene
947 Causes Thelytokous Parthenogenesis, the Defining Feature of the Cape Honeybee Apis
948 mellifera capensis. Curr. Biol. 30: 2248-2259.e6.

bioRxiv preprint doi: https://doi.org/10.1101/2022.04.27.489735; this version posted April 29, 2022. The copyright holder for this preprint (which was not certified by peer review) is the author/funder, who has granted bioRxiv a license to display the preprint in perpetuity. It is made available under aCC-BY 4.0 International license.

https://doi.org/10.1016/j.cub.2020.04.033

Zeileis A., and G. Grothendieck, 2005 zoo: S3 Infrastructure for Regular and Irregular Time Series. J. Stat. Softw. 14: 1–27. https://doi.org/10.18637/jss.v014.i06

Zhou Q., J. Zhang, D. Bachtrog, N. An, Q. Huang, *et al.*, 2014 Complex evolutionary trajectories of sex chromosomes across bird taxa. Science 346: 1246338. https://doi.org/10.1126/science.1246338

Zhou C., 2022 *YaHS: yet another Hi-C scaffolding tool*.